BUTTERWORTH HEINEMANN

Prediction of turbulent thermal convection in concentric and eccentric horizontal annuli

S. Kenjereš and K. Hanjalić
Faculty of Applied Physics, Delft University of Technology, The Netherlands

Natural convection in horizontal concentric and eccentric annuli with heated inner cylinder has been studied using several variants of single-point closure models at the eddy-diffusivity and algebraic-flux level. The results showed that the application of the algebraic model for the turbulent heat flux $\overline{\theta u_i}$, derived from the differential transport equation and closed with the low-Reynolds number form of transport equations for the kinetic energy k, its dissipation rate ϵ, and temperature variance $\overline{\theta^2}$, reproduced well the experimental data for mean and turbulence properties and heat transfer over a range of Rayleigh numbers, for different overheatings and inner-to-outer diameter ratios. The application of the extended algebraic turbulence models proved to be crucial for predicting the flow pattern and wall heat transfer at transitional Rayleigh numbers, where substantial turbulence persists only in a narrow plume above the heated inner cylinder, with laminar flow, or even stagnant fluid, prevailing in the remainder of the annuli.

Keywords: natural convection; annulus; turbulence modeling

Introduction

Natural convection in horizontal annuli with differentially heated inner and outer cylinders is characterized by a qualitatively different density stratification in the upper and lower domains, which imposes a strong variation of flow properties and a consequent nonuniformity of the heat transfer on the surrounding walls. Accurate prediction of the local fluid and wall temperature and heat transfer is often a major prerequisite for ensuring optimum design and operating safety in many industrial applications of annular flow passages, such as nuclear reactors, electronic cooling, inert gas insulation of high-voltage electric cables, cylindrical solar collectors. Until recently, such information was possible to obtain by experiment only. The developments in statistical turbulence modeling and methods for large-eddy simulation (LES) over the past few decades offered new prospects of numerically predicting flow and heat transfer details in new situations. However, a number of problems concerning the modeling of various turbulence interactions, be it for the full spectrum as implied by the single-point closure models, or for its high-wave number part required by the LES, remain to be resolved before these techniques can be widely employed for industrial applications. The present paper aims to contribute to that resolution: it discusses performances of several variants of statistical models in reproducing specific features of a buoyant flow and heat transfer in concentric and eccentric annuli at various conditions, and it recommends an algebraic model that can be employed for engineering predictions.

It has been shown in some of the very first experiments in horizontal annuli with inner and outer walls at different temperatures that several flow patterns and regimes may exist in different regions of an annulus: fully stagnant fluid in the stable stratified domain, turbulent plume above the heated surface, and laminar and transitional flow in between (e.g., Grigull and Hauf 1966; Lis 1966). The extent of various patterns depends on the ratio of the inner-to-outer cylinder diameters, heating rates, fluid properties, and other parameters. More recent experiments yielded new information about the field variables, primarily on the distribution of the mean temperature in the fluid and of Nusselt number around the cylinders circumference (e.g., Kuehn and Goldstein 1976, 1978; Bishop 1988; McLeod and Bishop 1989). These experiments, as well as others, showed that only in laminar cases up to $\mathrm{Ra}_L \approx 10^5$ (based on the gap width $L = (D_o - D_i)/2$ and temperature difference of the inner and outer cylinder $\Delta T = T_i - T_o$), the recirculating motion occupied the whole annulus. For a range of Rayleigh numbers considered from 2.5×10^6 to $\approx 1.0 \times 10^9$, the turbulence appears only in the upper region of the annulus in the plume above the heated inner cylinder, whereas a large portion of the flow below the cylinder remains nonturbulent and virtually stagnant, unaffected by the vigorous movement and fluctuations in the upper part. The stagnant region becomes progressively larger as the Ra number increases. This is to be expectaded, because the increased turbulence intensity causes a stronger mixing and momentum exchange above the heated inner cylinder. On the other hand, the stable stratification below the heated inner cylinder suppresses any movement and turbulence that might be convected downward, or possibly generated by shear deformation due to the mean flow motion, if extended from above into this region. Lis reported that the first signs of turbulence, isolated in small pockets adjacent to the outer cylinder and displaced on either one or both sides of the stagnation point, seemed to appear at Rayleigh number Ra_{D_i} (based on the inner cylinder diameter D_i) of about 1.4×10^6. Kuehn and Goldstein (1978) identified the onset of turbulence with the appearance of irregularity of the interferogram fringe patterns, which they detected at Ra_L around 1.5×10^6. At $\mathrm{Ra}_L = 1.6 \times 10^7$, they found that the upper part of the plume was fully turbulent. Persistent turbulence, occupying the entire plume and substantial portions

Address reprint requests to Prof. K. Hanjalić, Faculty of Applied Physics, Delft University of Technology, Lorentzweg 1, 2628 CJ Delft, The Netherlands.

Received 7 February 1995; accepted 16 June 1995

Int. J. Heat and Fluid Flow 16: 429–439, 1995

655 Avenue of the Americas, New York, NY 10010

0142-727X/95/$10.00
SSDI 0142-727X(95)00051-Q

of the boundary layer on the outer wall, with still laminar flow over the inner cylinder, was detected at $Ra_L \approx 2 \times 10^7$ and at somewhat higher values. It was only at $Ra_L = 8 \times 10^7$ that the boundary layer at the top of the inner cylinder became also turbulent.

More recently McLeod and Bishop (1989) provided new evidence on the nature of the flow regime in natural convection in an annulus of a similar configuration. From the analysis of the frequency spectrum of the temperature variance, obtained by hot wire, they found that only for $Ra_L \geqslant 10^9$ the fluctuations showed a broad band of frequencies, which they identified with fully turbulent regime. At lower Ra numbers, the observed spectrum recording showed low-frequency large spikes, which they associated with the laminar oscillations or transitional regime. Based on the visual observation and on the oscillograms of the temperature variance signal at several positions in the plume, McLeod and Bishop postulated physical models of the flow regimes at different Rayleigh numbers in the range from 10^7 to 10^9.

Another feature, particularly found by experiments at higher Rayleigh numbers, is the flow stratification and near uniformity of the temperature field over a large portion of the annuli central region, except, of course, very close to the walls within the thin boundary layers. This feature is particularly noticeable at high Ra numbers in the horizontal cross section at the annuli midheight (at 90°, measure from the vertical axis) where the flow structure resembles that in a side-heated vertical cavity. Almost constant temperature also appears in the vertical cross section above the heated cylinder (0°) at higher Ra numbers, where a strong unstable stratification generates a vertical plume and causes intensive vertical turbulent mixing, akin in some respects to the turbulent Benàrd convection between horizontal plates heated from below. At cross sections between 0 and 90° the temperature profiles exhibit inversion as a consequence of the recirculating motion.

Despite noted inhomogeneity of the flow structure and a variety of regimes, most of the past application-oriented research has been directed toward establishing *a general* correlation for heat transfer in term of Grashoff (or Rayleigh) and Prandtl numbers. As a result, a number of expressions of varying complexity can be found in literature that disagree with each other, as shown in Bishop (1988). More recent efforts tend to account for new experimental evidence and have been aimed at extending the heat transfer correlation by incorporating some new parameters, in addition to the Ra and Pr numbers. It has been recognized that the position of the laminar-to-turbulent transition, the extent of turbulence in annuli space, and the maximum turbulence intensity, all affecting the total heat transfer, also depend on the cylinders' diameter ratio for the same gap width, and, according to the results of McLeod and Bishop (1989), also on the relative overheat ratio ("expansion number") $\beta\Delta T$. For these reasons, more recent attempts to correlate heat transfer data have aimed at a correlation in a more general form $Nu = f(\mathrm{Ra}, \mathrm{Pr}, D_i/D_o, \beta\Delta T, \ldots)$, e.g., McLeod and Bishop. Bearing in mind the complexity of the flow structure, it is not surprising, however, that the heat transfer correlations proposed by various authors on the basis of experimental investigations in essentially different experimental environments (with, e.g., different radiative effects, uncontrolled heat losses, etc.), differ substantially in between and produce different heat transfer coefficients for nominally the same flow situations.

Even if a consensus on a correlation for the average Nusselt number is reached, it is unlikely that a usable general expression can be established for the local heat transfer coefficient and its distribution. Of course, such information can be obtained from experiments for a particular situation. Field computations of the temperature and velocity, either by direct or large-eddy numerical simulations or statistical modeling, will most certainly become an alternative route, offering much more flexibility, once the meth-

Notation

C	empirical coefficients in the turbulence model
e	eccentricity of the inner cylinder
f_μ, f_ϵ	dumping functions in the turbulence model
g_i	gravitation vector
h	heat transfer coefficient
k	kinetic energy of turbulence
K_{eq}	normalized Nusselt number, $\mathrm{Nu}/\mathrm{Nu}_{cond}$ ("equivalent thermal conductivity")
l_ϵ	turbulence length scale $k^{3/2}/\epsilon$
L	annulus width $(D_o - D_i)/2$
Nu	Nusselt number based on the cylinder diameter hD/λ
Nu_{cond}	normalization parameter $2/\ln(D_o/D_i)$
Pe	Peclet number RePr
Pr	Prandtl number ν/α
r	dimensionless radial coordinate $(2R - D_i)/(D_o - D_i)$
R	radial coordinate and thermal/mechanical turbulence time scale ratio τ_θ/τ
Ra	Rayleigh number
Ra_{D_i}	Rayleigh number based on D_i, $\beta g \Delta T D^3/\nu\alpha$
Ra_L	Rayleigh number based on L, $\beta g \Delta T L^3/\nu\alpha$
Re_t	turbulence Reynolds number $k^2/\nu\varepsilon$
T	mean temperature
T_c	reference temperature scale $(= \Delta T)$
ΔT	temperature difference $T_i - T_o$
u_i	turbulent fluctuation of the velocity vector
U_i	mean velocity vector
U_c	reference velocity scale $(\beta g \Delta T \nu)^{1/3}$
$\overline{u_i u_j}$	turbulent stress tensor
$\overline{\theta u_i}$	turbulent heat flux vector
x_i	space coordinates

Greek

α	temperature diffusivity
β	thermal expansion factor
ε	dissipation rate of the turbulence kinetic energy
ε_θ	dissipation rate of the temperature variance
η	empirical coefficient, Equation 1
$\tilde{\varepsilon}$, $\tilde{\varepsilon}_\theta$	homogeneous parts of ε and ε_θ
$\overline{\theta^2}$	temperature variance
λ	thermal conductivity
μ	dynamic viscosity
ν	kinematic viscosity
ξ	empirical coefficient, Equation 1
ρ	fluid density
τ	mechanical time scale of turbulence k/ε
τ_θ	thermal time scale of turbulence $\overline{\theta^2}/2\varepsilon_\theta$
ϕ	angle around annulus, measured downward from the top

Indices

c	characteristic, reference value
i	inner, hot cylinder
o	outer, cold cylinder
t	turbulent

ods are developed to a mature stage. Direct numerical simulation (DNS) by Fukuda et al. (1990) provided valuable insight into the flow pattern and regimes, as well as into the influence of various parameters on the flow structure. However, because of the extreme requirements for computing resources, these computations are limited to low Ra numbers (at present less than 10^6). These Ra numbers are insufficient to attain a persistent turbulence even in the top portion of the hot plume, where the conditions for turbulence existence are most favorable. Fukuda et al. obtained fluctuations of the velocity and temperature that appeared to be similar to those found by experiments, which they identified with turbulence and calculated their rms values, as well as their spectra. However, the numerical recordings seem to resemble more the oscillatory patterns akin to those detected earlier by optical methods in an unstable laminar flow prior to transition or in the early stage of transition. Indeed, the authors cautioned on the insufficient numerical resolution of the fine-scale fluctuations due to the restriction upon the numerical grid, resulting in incomplete simulation of the dissipation and, consequently, in an overestimate of the turbulence intensity. Direct numerical simulations at higher Ra numbers, which would yield valuable information about the turbulence structure in a fully turbulent regime, remain to be performed.

For the computation of natural convection at high Rayleigh numbers two methods are now available: the LES and the single-point turbulence closure modeling. Recent LES by Miki et al. (1993) of a case with a relatively high Ra_L number of 1.18×10^9 indicated that this method may serve in the future as an alternative to the DNS for higher Ra numbers, but the agreement with experiments, which the authors characterized as "reasonable," revealed that some serious uncertainties remain regarding the subgrid modeling and treatment of the wall boundary conditions. Because of these uncertainties, as well as the continuing excessive requirements for computing resources, the LES technique, although very promising for providing much needed information, is still inadequate for industrial computation.

At present, statistical modeling remains the only method for computing the velocity and temperature distribution and the wall heat transfer in unknown situations (e.g., Hanjalić 1994). For isothermal pressure- and shear-dominated turbulent flows, as well as for the forced convection, the single-point turbulence models and numerical computations seem to be gaining ground and credibility for wider industrial applications. However, the predictions of natural convection have thus far yielded much less satisfaction because of uncertainties in accounting for some specific effects, such as the buoyancy-induced interaction between the velocity and temperature field, counter-gradient diffusion, viscid–inviscid interactions, and others, requiring generally a higher level of modeling, as compared with isothermal flows or forced convection. For instance, because of a strong flow stratification in the central zone and a high anisotropy of the turbulence field, the simple gradient diffusion hypothesis, which relates the turbulent heat flux component to the aligned component of the temperature gradient, as implied by the standard, scalar eddy-diffusivity hypothesis, can mimic neither the strong cross-diffusion nor the mutual interaction between the mean velocity and nonuniform and strongly anisotropic buoyant turbulence field. For that reason, a higher-order modeling of the turbulent heat flux is required, at least at the level of algebraic specification in terms of the vector temperature gradient, mean flow deformation, and temperature variance.

A variety of flow patterns and the coexistence of stagnant fluid, laminar, transitional, and turbulent regimes within the same flow domain over a wide range of Rayleigh numbers poses another challenge to the modeling and computational methods. Any model that pretends to mimic the flow and turbulence field, should account for the low Reynolds/Peclet number effects that are not necessarily related to the near-wall molecular sublayer. The model is also expected to reproduce the interactions between the laminar-like motion and turbulence adequately. Of course, no single-point statistical turbulence model can be expected to describe the onset and development of instability of the laminar motion or the oscillations detected in the transitional regimes. However, the prediction of distribution of average turbulence intensity and associated turbulent stresses and heat flux components in transitional regions and a form of continuous transition from the laminar to the turbulent regime are the essential prerequisites for predicting the heat transfer distribution along the bounding walls.

The present paper reports on the modeling and computational study of the natural convection in concentric and eccentric annuli by means of several variants of the algebraic model, based on the expression for turbulent heat flux $\overline{\theta u_i}$ obtained by truncation of the second-moment transport equation for this correlation. Various levels of closure include the low-Re number form of the k-ε model, but also a version in which the differential transport equations are solved for the temperature variance $\overline{\theta^2}$ and its decay rate ε_θ. All versions have been tested earlier in a study of rectangular enclosures of different aspect ratios and different boundary conditions (Hanjalić et al. 1995; and Kenjereš and Hanjalić 1995). The present study focuses on annuli for a range of Ra_L numbers from 10^6 to 10^9 for which the experimental and LES data are available in the literature. Over the range considered, the levels of turbulence were markedly different. For the verification of numerical accuracy, several cases of laminar flow at lower Ra numbers were also considered.

Adopted turbulence model

A general algebraic expression for the turbulent heat flux vector, derived from the modeled differential equation for $\overline{\theta u_i}$ by omitting the transport terms, can be written as follows:

$$\overline{\theta u_i} = -C\frac{k}{\varepsilon}\left(\overline{u_i u_j}\frac{\partial T}{\partial x_j} + \xi\overline{\theta u_j}\frac{\partial U_i}{\partial x_j} + \eta\beta g_i\overline{\theta^2}\right) \tag{1}$$

The closure of Equation 1 can be accomplished by solving the transport differential equations for the turbulence energy k and its dissipation rate $\varepsilon = \nu\overline{(\partial u_i/\partial x_j)^2}$ and for the temperature variance $\overline{\theta^2}$ and its dissipation rate $\varepsilon_\theta = \alpha\overline{(\partial\theta/\partial x_j)^2}$. The four scalar variables define the characteristic mechanical and thermal turbulence time scales $\tau = k/\varepsilon$ and $\tau_\theta = \overline{\theta^2}/2\varepsilon_\theta$, which can be employed to model various terms in the equations set. The four transport equations are also expected to account for the turbulence evolution and compensate in part for disregarding the individual transport of turbulent flux and stress components. Together with expression 1 and the analog algebraic expressions for turbulent stresses $\overline{u_i u_j}$, these four scalar transport equations, extended to account for low-Re- (or low Pe-number effects, if the Prandtl number is very different from unity) constitute the algebraic stress/flux model that, in our opinion, presently yields the optimum level of modeling of natural convection in complex geometries.

Of the four transport equations mentioned, the equation for ε_θ poses most uncertainties. This equation essentially governs the transfer of the temperature variance down the turbulence spectrum and its ultimate molecular destruction and is influenced by both the mechanical and thermal turbulence scales. Its dynamics are also affected by the deformation of both the mean velocity and mean temperature fields so that the transport equation contains at least twice as many terms and associated empirical coefficients as the equation for the mechanical dissipation rate ε. For these reasons, in most published works on modeling natural

convection, the solving of the transport equation for ε_θ is avoided by employing the simple expression $\varepsilon_\theta = \varepsilon\overline{\theta^2}/(2kR)$, which rests on the assumption that the ratio of the thermal to mechanical turbulence scale $R = \tau_\theta/\tau$ remains constant throughout the flow, or is expressed in terms of some known scalar properties of turbulence. Measurements and DNS of several types of buoyant flows indicate that the assumption of constant R is not justified (e.g., Shabbir and Taulbee 1990; Grötzbach and Wörner 1992). Our computations of several cases of natural convection in rectangular enclosures of different aspect ratios by solving all four transport equations also confirmed that R varies substantially over the flow domains and depends on the flow geometry and boundary conditions (Hanjalić 1994). However, in several flows considered it seems that the overall results are not very sensitive to the accurate specification of the ε_θ, although different values of R seem to be required for different flows in order to reproduce best the experimental or DNS results. In view of the mentioned uncertainties in closing the transport equation for ε_θ, but also encouraged by the satisfactory performance of the three-equation model in other geometries, we confine our discussion to the results obtained with the k-ε-$\overline{\theta^2}$ model and assumed R = const. The model consists of the following set of equations:

$$\frac{\mathrm{D}(\rho\overline{\theta^2})}{\mathrm{D}t} = D_\theta + 2\rho P_\theta - 2\rho\varepsilon_\theta \tag{2}$$

$$\frac{\mathrm{D}(\rho k)}{\mathrm{D}t} = D_k + \rho P + \rho G - \rho\varepsilon \tag{3}$$

$$\frac{\mathrm{D}(\rho\tilde{\varepsilon})}{\mathrm{D}t} = D_\varepsilon + C_{\varepsilon 1}\rho P\frac{\tilde{\varepsilon}}{k} + C_{\varepsilon 3}\rho G\frac{\tilde{\varepsilon}}{k} - C_{\varepsilon 2}f_\varepsilon\rho\frac{\tilde{\varepsilon}^2}{k} + 2\mu\frac{\mu_t}{\rho}\left(\frac{\partial^2 U_i}{\partial x_j \partial x_k}\right)^2 + S_l \tag{4}$$

where

$$P = -\overline{u_i u_j}\frac{\partial U_i}{\partial x_j}; \qquad G = -\beta g_i\overline{\theta u_i}; \qquad P_\theta = -\overline{\theta u_j}\frac{\partial T}{\partial x_j} \tag{5}$$

$$\tilde{\varepsilon} = \varepsilon - 2\nu\left(\frac{\partial(k)^{\frac{1}{2}}}{\partial x_n}\right)^2 \qquad D_\phi = \frac{\partial}{\partial x_j}\left(C_\phi f_\mu\rho\frac{k^2}{\tilde{\varepsilon}}\frac{\partial\phi}{\partial x_j} + \mu\frac{\partial\phi}{\partial x_j}\right) \tag{6}$$

$$S_l = \max\left[\left(0.83\left(\frac{l_\varepsilon}{l} - 1\right)\left(\frac{l_\varepsilon}{l}\right)^2\frac{\tilde{\varepsilon}^2}{k}\right), 0\right], \qquad l_\varepsilon = \frac{k^{3/2}}{\varepsilon},$$

$$l = 2.5x_n \tag{7}$$

Here P and G represent turbulence energy production by strain and buoyancy respectively, P_θ is the production of temperature variance, and D denotes the total diffusion term in which the turbulent part was modeled by the simple gradient hypothesis. S_l is the length scale correction in the wall vicinity.

A consistent approach would require the application of an analog algebraic model for the turbulent stress $\overline{u_i u_j}$. However, an accurate prediction of the normal stress components, $\overline{u_i u_i}$, where the algebraic approach is superior, did not prove to be very important, at least in two-dimensional enclosures (Hanjalić 1994). To keep the model relatively simple, we employed the standard eddy-viscosity expression for the computation of turbulent stresses:

$$\overline{u_i u_j} = \frac{2}{3}k\delta_{ij} - \nu_t\left(\frac{\partial U_i}{\partial x_j} + \frac{\partial U_j}{\partial x_i}\right)$$

where

$$\nu_t = 0.09 f_\mu k^2/\tilde{\varepsilon} \tag{8}$$

The equations were solved over the whole flow domain up to the wall were the exact boundary conditions ($T = T_w$, all other properties equal to zero) were employed.

For the computation of natural convection, where both laminar and turbulent regions may exist in the same flow domain, the model is required to reproduce a gradual transition from one to another regime, not only across the molecular wall sublayer, but also at the edge of turbulence zones away from the wall. In the latter case, the turbulent fluctuations decay freely under the action of molecular forces. This process is physically different from the turbulence damping in the near-wall region, where the molecular effects are mixed with the eddy splatting due to the wall blockage and pressure reflection. A consistent approach would require separate modeling of these effects, as practiced in some recent second-moment closure models. In the present work, we have followed the low-Re-number modifications introduced for isothermal wall flows where the damping functions have been expressed solely in terms of the turbulence Re number. For flows with Pr around unity, the low Re-number modifications of the k and ε equations appeared to suffice and no direct modifications of the $\overline{\theta^2}$ equation were found necessary. We adopted the damping functions of Jones-Launder (1972), modified by Launder and Sharma (1974): $f_\mu = \exp[-3.4/(1 + \mathrm{Re}_t/50)^2]$ and $f_\varepsilon = 1 - 0.3\exp(-\mathrm{Re}_t^2)$, which were reported to reproduce reasonably well the distribution of mean velocity and turbulence energy across the viscous sublayer into the fully turbulent outer wall region, as well as (although with less success) the laminarization of accelerating boundary layers. An additional argument in favor of this model is its successful application (although with the nonisotropic eddy diffusivity) to the prediction of natural convection in a side-heated 5:1, two-dimensional (2-D) enclosure, reported by Ince and Launder (1989). We also followed their positive experience with the inclusion of the length-scale wall correction term S_l in the dissipation equation, attributed to Yap. Our previous computations of rectangular cavities showed that good agreement with experiments can be achieved without this correction, although with somewhat different values of the coefficient C. However, it was found that its inclusion prevents excessive growth of the length scale slope in the wall vicinity and thus far improves the predictions in the near wall regions, particularly close to flow separation and impingement, and contributes to the robustness of the numerical method.

The algebraic model for the turbulent heat flux can be truncated at different levels, depending on how many and what terms in expression 1 are retained. In the simplest version, Equation 1 reduces to the standard eddy-diffusivity model with isotropic exchange coefficient $\overline{\theta u_i} \alpha -k^2/\varepsilon(\partial T/\partial x_i)$. This model, known also as the simple gradient diffusion hypothesis, was found inadequate for free convection, because it expresses the heat flux component in terms of only the aligned component of the mean temperature gradient. A more general approach, the general gradient diffusion concept, is to employ the complete form of the first term in expression 1, which implies, in fact, a tensorial form of eddy diffusivity. This approach was found to substantially improve the prediction of natural convection in tall cavities and at a vertical heated plate. The inclusion of the second term in Equation 1 will also account for the interaction of the turbulent heat flux and mean flow deformation, which may be important in the near-wall regions. The last term represents the contribution to $\overline{\theta u_i}$ due to the temperature variance interacting with the gravitational field. This term is particularly important for predicting pure buoyant flows in nearly uniform temperature field, such as a mixed layer above a heated surface, because it becomes the sole generator of the turbulent heat flux. Expressing the temperature

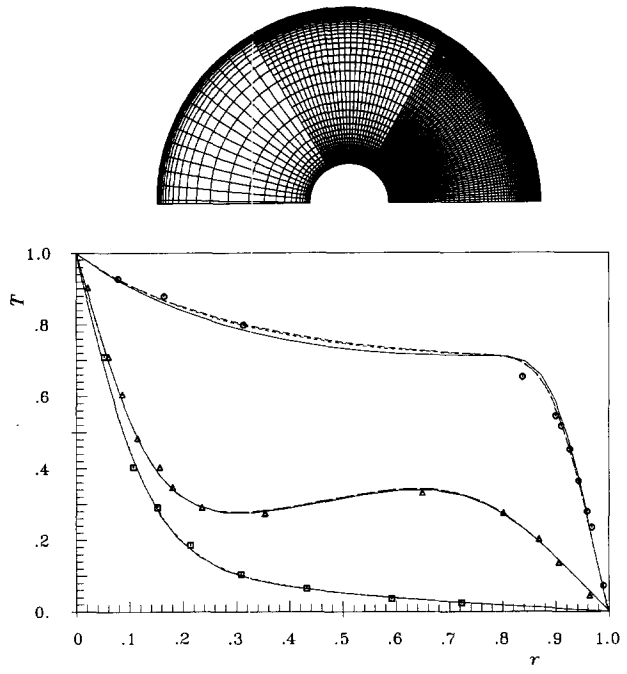

Figure 1 Dimensionless temperature profiles for laminar regime in a concentric annulus, $D_o/D_i = 2.6$, $Ra = 5 \times 10^4$; lines: multigrid computations with three grid levels, 30×40, 60×80, and 120×160; symbols: experiments of Kuehn and Goldstein (1978), $\circ - \phi = 0°$, $\Delta - \phi = 90°$, $\square - \phi = 180°$

variance in terms of the mean temperature gradient $\overline{\theta^2}\alpha - C_\theta(k\overline{\theta u_j}/\varepsilon)(\partial T/\partial x_j)$, as often practiced in modeling the forced convection, is inadequate in buoyant flows in absence of temperature and velocity gradient, or when the temperature profile exhibits inversion. The solution of the differential transport equation for $\overline{\theta^2}$ seems, therefore, very appropriate, particularly bearing in mind that the closure and solution of this equation, except for defining its sink term ε_θ, as discussed earlier, does not require a special effort.

In the present paper, we discuss results obtained by the three-equation, k-ε-$\overline{\theta^2}$ model with the complete algebraic expression 1 for the heat flux. Most computations presented have been obtained for $R = 0.5$, the value found to hold reasonably well in some simple forced-convection flows. Some other values have been tested, such as $R = 0.25$, as discussed later.

The following values of the coefficients have been adopted: $C = 0.1$, $C_k = C_\theta = 0.09$, $C_\varepsilon = 0.07$, $C_{\varepsilon 1} = C_{\varepsilon 3} = 1.44$, $C_{\varepsilon 2} = 1.92$, $\eta = \xi = 0.6$. Most of the coefficients are well established and require no further comments. The exception is the coefficient C in Equation 1, which is still under scrutiny. It should be noted that the adopted value of 0.1 is the optimum for the considered annuli flow. The value of 0.2, found as an optimum for a range of rectangular cavities, reproduced also reasonably well the high Ra number annulus, but generated too strong turbulence levels at $Ra \approx 10^7$. Also, for comparison some results obtained with the generalized gradient diffusion hypothesis (denoted as GGDH) are presented.

Numerical method

Numerical computations were performed by a version of finite volume Navier–Stokes solver for 2-D flows, written in a curvilinear coordinate system with Cartesian velocity components (Demirdžić and Perić 1990). A collocated grid, clustered toward the walls in radial and uniformly spaced in circumferential direction was employed with typically 120×160 grid points. The convection terms were computed by using the first-order upwind differencing scheme; whereas, the diffusion terms were treated by central differencing. Some tests with hybrid schemes for the convection indicated that a higher weighting toward the central differencing deteriorates the scheme stability, without any effect on the computational accuracy for the grid considered. The solutions were obtained by false time marching, employing the Stone's strongly implicit iterative ILU method. SIMPLE algorithm was used for the treatment of the pressure field. For laminar cases, the multigrid acceleration was employed with three grid levels, 30×40, 60×80, and 120×160 CV, shown in parallel in Figure 1. However, in the case of turbulent flows, particularly at lower Ra numbers, the coarse grid tends to damp the turbulence, so the mutigrid approach did not prove to be very beneficial. With a fine grid, the convergence was slow, requiring in some cases for higher Ra numbers as many as 30,000 iterations to achieve a satisfactory solutions with residuals for mean momentum, energy, and pressure field each less than 10^{-8}. Slow convergence is probably a consequence of inadequacy of the SIMPLE and similar procedures for buoyancy-dominated flows, because this method is based on pressure–velocity coupling, which does not account directly for a strong effect of the temperature field. However, satisfactory convergent solutions have been obtained in all cases considered. For the present work focused on testing turbulence models, no great need was felt to introduce a more efficient scheme accounting directly for the temperature–velocity coupling, such as that proposed by Galpin and Raithby (1986), although for more complex and three-dimensional (3-D) geometries this may prove to be necessary.

Laminar flow computations

Numerical verifications of the method were performed by first computing several cases of laminar flow in both concentric and eccentric annuli. Selected were those cases investigated experimentally by Kuehn and Goldstein (1978) at $Ra_L \approx 5 \times 10^4$ with vertical eccentricity $e/L = 0$, $\approx +2/3$ and $-2/3$. The computed results show excellent agreement with the experiments both qualitatively, exhibiting identical flow patterns as recorded by interferometer (Figure 2 in the paper of Kuehn and Goldstein 1978), and quantitatively in the distribution of temperature and heat transfer coefficient. A selection of results is shown in Figures 2–4, each showing the isotherms, streamlines, and the Nusselt number distribution around the inner and outer cylinder walls. Several interesting features, detected in experiments, are fully reproduced, such as the existence of a boundary all around the outer cylinder when the inner cylinder is displaced downward or its absence on the bottom part in the case when the inner cylinder is moved upward. The plume disappearance in the latter case with symmetric secondary roll-cells above the inner cylinders is also well captured. The computed distribution of the Nusselt number, presented in terms of effective conductivity, is also very well reproduced in all three cases, except for some discrepancy in the plume impingement on the outer cylinder in the cases with $e/L = 0$ and 0.652 and in the central portion of the outer cylinder for $e/L = 0.623$. These discrepancies show no consistency and could not be explained. However, the overall agreement can be regarded as satisfactory, confirming a full credibility into the applied numerical method.

Model validation and results for turbulent flows

Concentric annuli

To demonstrate the performances of the adopted model, two sets of independent experimental data were simulated numerically:

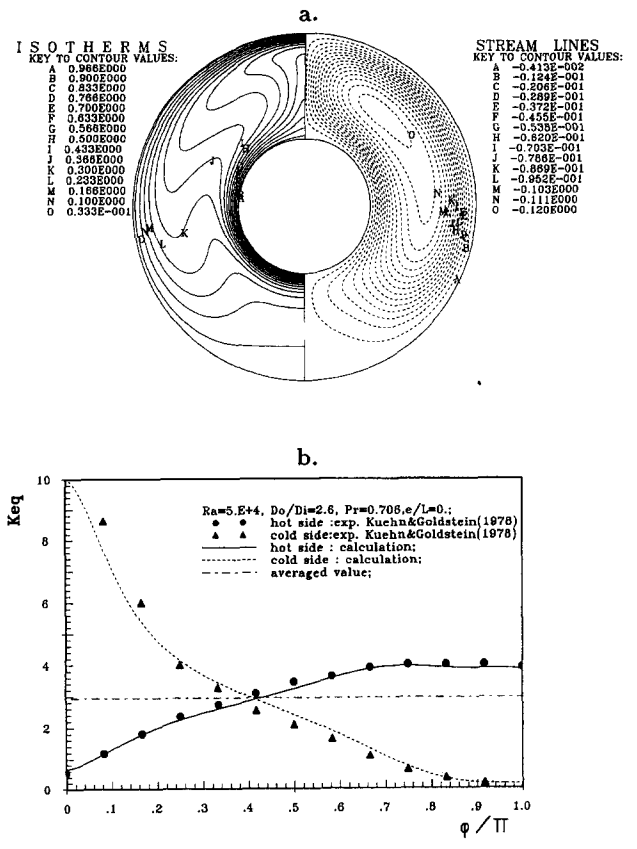

Figure 2 Computation of laminar flow in a concentric annulus, $D_o/D_i = 2.6$, $\mathrm{Ra} = 5 \times 10^4$, (a) isotherms and streamlines; (b) normalized Nusselt numbers along the inner and outer cylinders

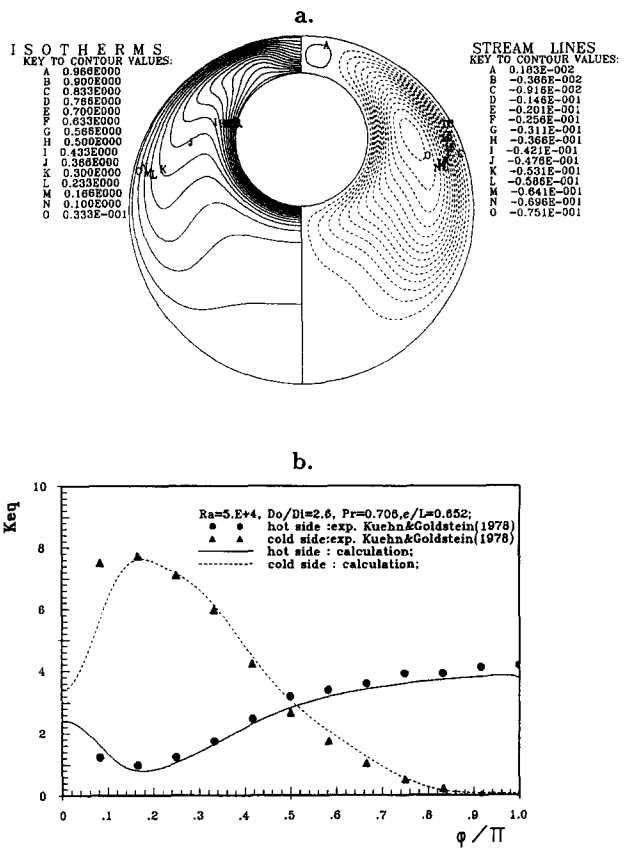

Figure 3 Computation of laminar flow in an eccentric annulus, $D_o/D_i = 2.6$, $e/L = 0.652$, $\mathrm{Ra} = 5 \times 10^4$; (a) isotherms and streamlines; (b) normalized Nusselt numbers along the inner and outer cylinders

the experiments of Kuehn and Goldstein (1978), and McLeod and Bishop (1989) (also Bishop 1988). Selected were those cases for which more detailed experimental data were reported in the literature. The first authors considered an annulus with the diameter ratio $D_o/D_i = 2.6$ and covered the Ra_L numbers up to 7.7×10^7. Because of the limitations of the optical technique used, the highest Ra number for which they measured the temperature distribution and the local heat transfer was 2.5×10^6, and we selected this case for model validation. Bishop (1988) and McLeod and Bishop (1989) used an annulus with $D_o/D_i = 4.85$ and reported measurements for $\mathrm{Ra} = 1.2 \times 10^7$ to 1.2×10^9. No data, experimental or numerical, for eccentric annuli at higher Ra numbers with turbulent regime were found in literature, and the results are presented and discussed without comparison.

Flow pattern. The computed streamlines and contours of isotherms and some of the turbulence properties, shown in Figures 5 and 6 for two Ra numbers, 2.5×10^6 and 1.18×10^9, each corresponding to a different diameter ratio, illustrate typical flow patterns for the turbulent natural convection in an annulus. Both cases contain regions with established turbulence, but also both have stagnant regions below the inner cylinder with the cold stagnant fluid. The streamlines and the temperature contours for $\mathrm{Ra} = 2.5 \times 10^6$, Figure 5a, resembles those for the laminar regime, as recorded by interferograms by Kuehn and Goldstein (1978) at lower Ra numbers (10^5–10^6). However, there are important differences in the thin boundary layers on both cylinders, which influence the mean temperature distribution and, consequently, the local heat transfer coefficient, as discussed later. At the higher Ra number, the flow pattern has similar general features, characterized by the heated plume above the inner cylinder, impinging on the outer cylinder in the upper central region and spreading toward both sides, inducing a strong circular motion. However, the major difference is in the extent of the recirculating zones: it is obvious that an increase in the Ra number causes more intensive mixing, which reduces the recirculation to the smaller region in the upper domain, leaving a larger portion of the annulus (almost complete lower half of it in the case of $\mathrm{Ra} = 1.18 \times 10^9$) fully stagnant and unaffected by heating. The turbulence levels are, of course, different, as illustrated by the plot of the contours of turbulence properties in Figures 5b–5d and 6b–6d. The temperature variance $\overline{\theta^2}/\Delta T$ showed very different distributions for the two cases, although, when normalized with the hot-to-cold wall temperature difference, ΔT, the maximum values seem to be very close. The turbulence intensities k/U_c^2, normalized with the buoyancy velocity scale $U_c = (\beta g \Delta T \nu)^{1/3}$, showed a substantial difference, not only in distribution, but also in the relative magnitude, indicating that the employed velocity scale is inadequate for scaling turbulence properties in the whole annulus cross section. Similar conclusions can be drawn for the turbulent heat flux components, Figures 5b and 6b, which show a marked concentration of both components in the vicinity of the inner heated cylinder. The maximum normalized values are reasonably close to each other in the two cases; whereas, the distributions are dissimilar. At a lower Ra number and a smaller gap width, the influence of the hot wall on the turbulence fluctuations stretches much into the boundary layer along the outer cold cylinder. In contrast, at higher Ra numbers and wider annulus gaps, much more intensive turbulence fluctuations occur close to the heated cylinder, so that the gradients of all turbulence properties are much steeper in this region than in the boundary layer along the outer cylinder.

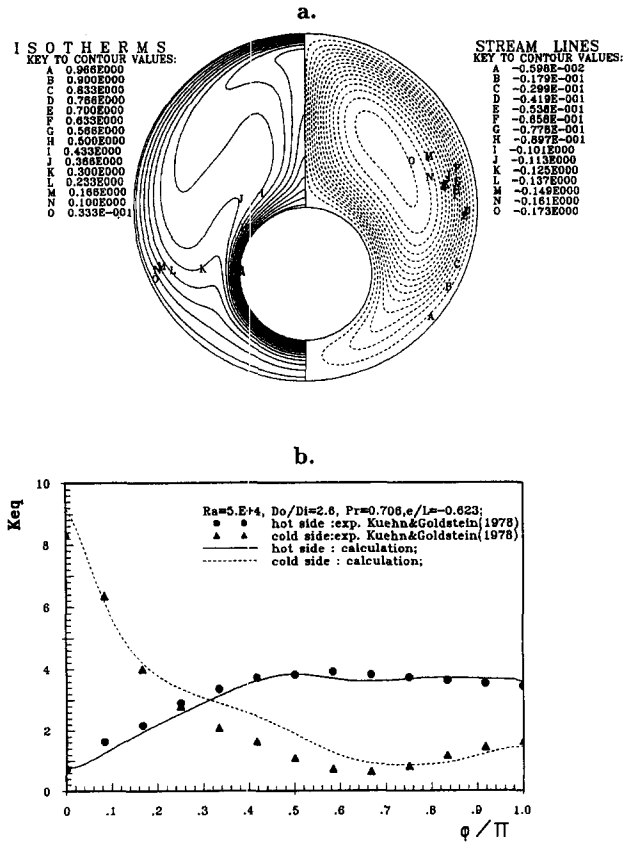

Figure 4 Computation of laminar flow in an eccentric annulus, $D_o/D_i = 2.6$, $e/L = -0.623$, $\mathrm{Ra} = 5\times10^4$, (a) isotherms and streamlines; (b) normalized Nusselt numbers along the inner and outer cylinders

Another representative of the turbulence field is the turbulent Re number $\mathrm{Re}_t = k^2/\nu\varepsilon$, shown in Figures 5d and 6d. At the lower Ra, the peak Re_t is about 200; whereas, at the higher Ra number, Re_t reaches a peak of about 2000. Some further indication of the turbulence field is illustrated by the plots of the length scales $k^{3/2}/\varepsilon$, normalized with the annulus gap L, shown on the right in Figures 5d and 6d.

Property distribution and local heat transfer. A better assessment of the model performances can be inferred from the comparison of the profiles of the mean and turbulence properties in selected cross sections of the annuli. First, the low Ra number case of Kuehn and Goldstein (1978) was considered. Figure 7 compares the temperature profiles computed with the described algebraic model for $\mathrm{Ra} = 2.5\times10^6$ for two values of the time scale ratios $R = 0.5$ and 0.25 (solid and dotted lines). Also presented are the results obtained by the GGDH model. Around this Ra number (in fact, above 1.5×10^6) Kuehn and Goldstein (1978) reported that there was no definite frequency of plume oscillation and that the flow tended to become more irregular with increasing Ra number, with more intensive fluctuations in the outer cylinder boundary layer. The chain lines show the results obtained by the general gradient diffusion hypothesis, with the turbulent heat flux expressed as $\overline{\theta u_i} = -C_\phi(k\overline{u_i u_j}/\varepsilon)\partial T/\partial x_j$, with $C = 0.15$ (Ince and Launder 1989), which could not maintain the turbulence: the flow laminarized regardless of the initial turbulence levels, and even with $C = 0.2$, so that the chain lines represent essentially laminar solutions. The success in predicting a partially turbulent regime with the algebraic model for the heat flux (the other set of curves) is probably because of the inclusion of the mean velocity, and, particularly, of the temperature variance (third, fourth, and fifth term in Equation 1). It is interesting that this model produced a persistent, although rather weak turbulence, with the peak turbulence Reynolds number of about 200 corresponding roughly to the turbulent-to-molecular viscosity

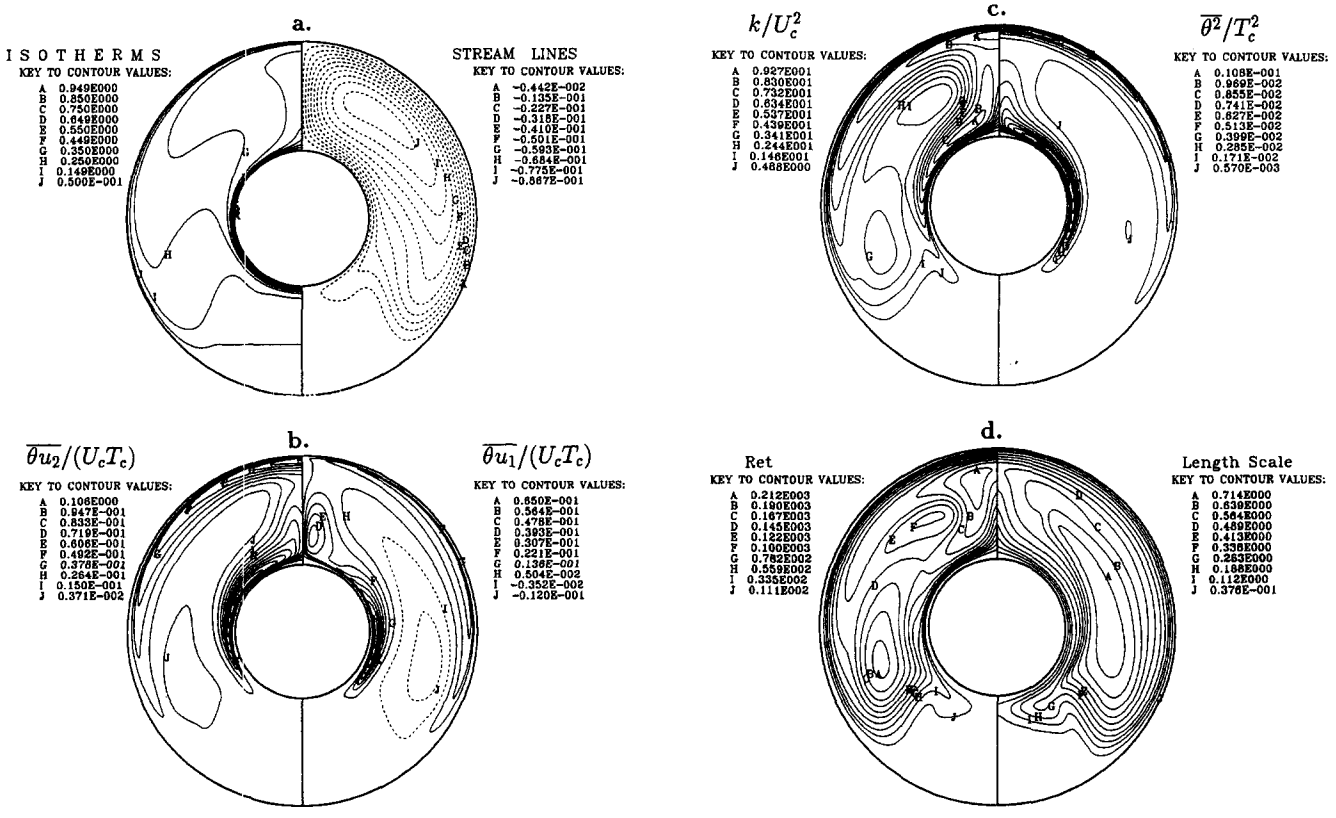

Figure 5 Computed contours of mean flow and turbulence properties in a concentric annulus, $D_o/D_i = 2.6$, $\mathrm{Ra} = 2.5\times10^6$

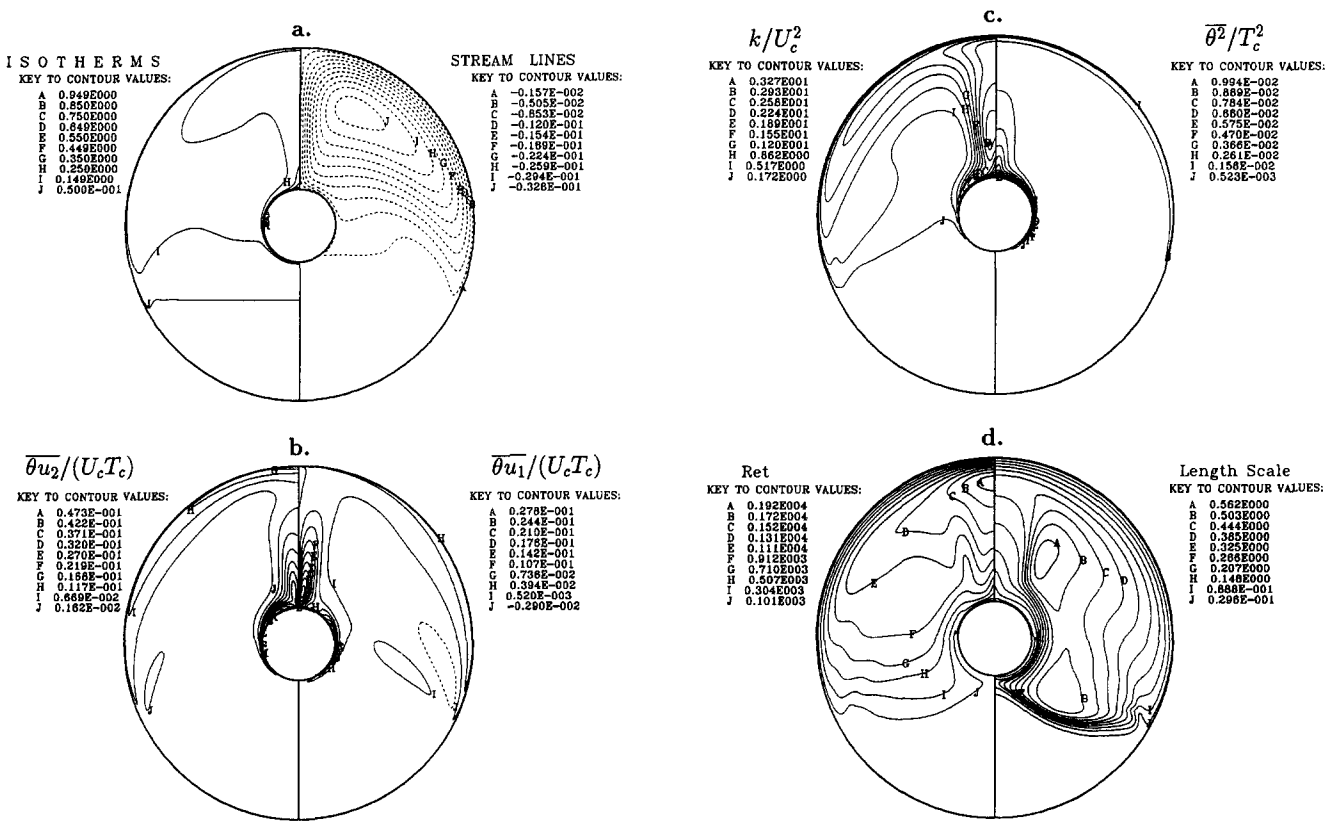

Figure 6 Computed contours of mean flow and turbulence properties in a concentric annulus, $D_o/D_i = 4.85$, $\mathrm{Ra} = 1.18 \times 10^9$

ratio of about 16. Consequently, the two models produced very similar results for the lower portion of the annuli where the flow remains laminar; e.g., angles 90° to 180°, (although not identical, because of the modification of the mean flow). However, this small turbulence, concentrated in the upper portion of the annuli brought about a substantial improvement of the agreement with experiments of both the temperature profiles and Nusselt number distribution, as shown in Figures 7 and 8 for $R = 0.25$. Slightly higher values of the Nusselt number on the upper portion of the inner cylinder were obtained with $R = 0.5$ (not shown). This suggests that the flow investigated experimentally by Kuehn and Goldstein at this Ra number did not retain the laminar pattern fully, but already had some established turbulence in the upper outer part of the cylinder, which modified the flow and influenced the Nusselt number. The average normalized Nusselt number ("equivalent thermal conductivity"), $K_{eq} = \mathrm{Nu}/\mathrm{Nu}_{cond}$ of 7.80 agrees very well with the experimental value of 7.88 of Kuehn and Goldstein; whereas, the laminar solution gave only 6.2, as shown in Figure 8. Note that $\mathrm{Nu} = hD/\lambda$ and $\mathrm{Nu}_{cond} = 2/\ln(D_o/D_i)$, (where h is the heat transfer coefficient, λ is the fluid conductivity, and D is the corresponding cylinder (inner or outer) diameter).

The influence of the increased Ra number on thinning the boundary layers and reducing the mean temperature in the bulk of the cross section area, shown in Figures 9–11, is very well reproduced by the algebraic model. Figure 9 shows the comparison of the temperature profiles for the highest considered Ra number of 1.18×10^9, with the two values of R, 0.5 and 0.25.

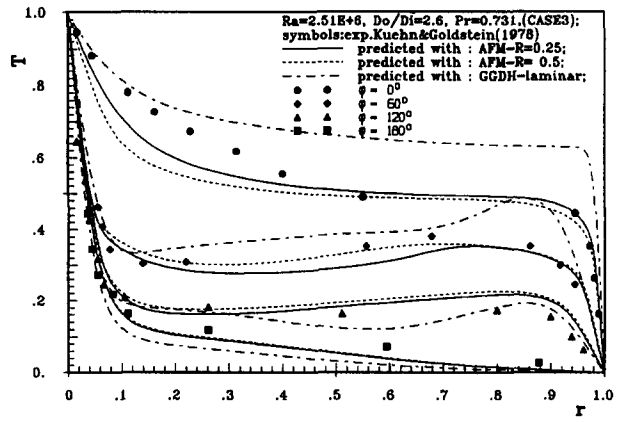

Figure 7 Dimensionless temperature profiles in a concentric annulus, $D_o/D_i = 2.6$, $\mathrm{Ra} = 2.5 \times 10^6$

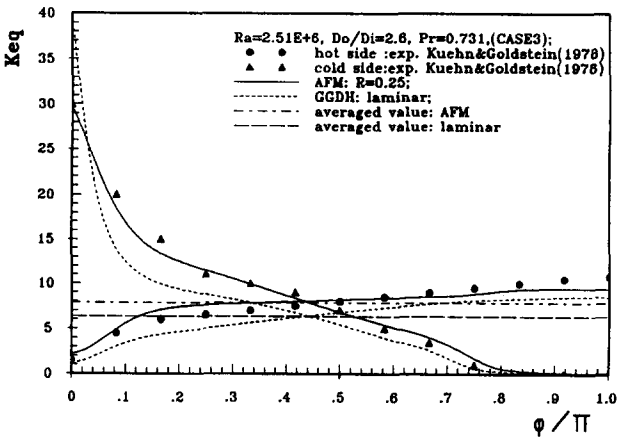

Figure 8 Normalized local Nusselt number around the inner and outer cylinder of a concentric annulus, $D_o/D_i = 2.6$, $\mathrm{Ra} = 2.5 \times 10^6$

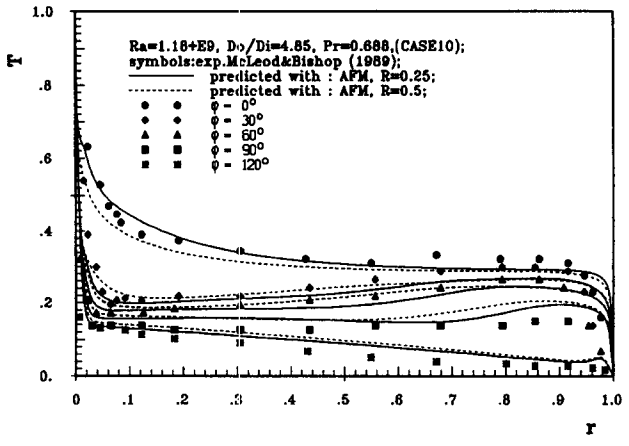

Figure 9 Dimensionless temperature profiles in a concentric annulus, $D_o/D_i = 4.85$, Ra = 1.18×10^9

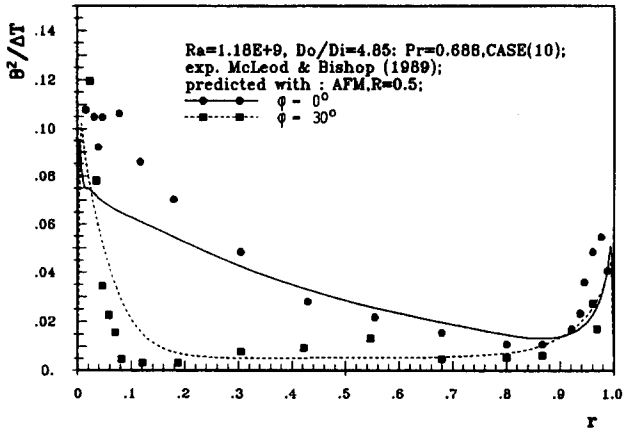

Figure 11 Dimensionless temperature variance in a concentric annulus, $D_o/D_i = 4.85$, Ra = 1.18×10^9 at the plume center, $\phi = 0°$ and at $\phi = 30°$

Both results agree well with the experiments, with a marginal advantage of $R = 0.5$. In this case, the complete plume remained turbulent affecting also the temperature profile close to the inner cylinder at 0°. As in the previous case, the model reproduced the temperature inversion and an apparent countergradient diffusion in the central part of the annulus at the angles between 30° and 90°. Figure 10 shows the computed distribution of the Nusselt number around both the inner and outer cylinders for the two values of R. Apart from much higher values of the K_{eq} numbers, the distribution looks similar to that of the previously discussed case at lower Ra number. The only difference is the region at the top of the inner cylinder at the plume separation, where now the K_{eq} number shows a peak, a sudden drop to a minimum, and a subsequent increase and leveling at an almost constant value over the much of the circumference. No experimental data are available for the local heat transfer coefficient. However, some indication can be obtained from the comparison of the averaged value with the heat transfer correlations. The averaged value of about 37, obtained with $R = 0.5$ agrees very well with the experimental results of McLeod and Bishop (1989); whereas, using $R = 0.25$ gives about 10% lower value.

Figure 11 shows the comparison of the computed and measured temperature variance distribution at two angles, 0° and 30°. The first case corresponds to the centerline of the plume. A drastic decrease in $\tilde{\theta} = \sqrt{\theta^2}$ at 30° in the whole annulus cross section, apart from the thin wall boundary layers indicates that the turbulence is mainly concentrated in the plume, with very little fluctuation outside it. The model with $R = 0.5$ reproduced this pattern reasonably well; whereas, $R = 0.25$ produced much worse agreement (not shown here). The results presented illustrate how sensitive the reproductions of the natural convection at transitional Ra numbers are when the turbulence remains confined to only a small region of the flow.

Average heat transfer coefficient. Several heat transfer correlations for horizontal annuli can be found in literature (Bishop 1988). Most of these are expressed in terms of an equivalent thermal conductivity K_{eq} as defined earlier. K_{eq} (or Nu) is usually correlated with Ra (or Gr) number for a range of Prandtl numbers and of diameter ratios. McLeod and Bishop (1989) also introduced the expansion number $\beta\Delta T$ as an independent parameter. Available correlations differ in between substantially yielding different values of the heat transfer coefficient for the same geometry and conditions. In addition to the form of the correlations, a major difference appears in the use of the characteristic dimension in defining the Rayleigh number, for which some authors use the gap width $L = (D_o - D_i)/2$; whereas, others prefer the diameter of the inner cylinder. Bishop compared his experimental results with several correlations and found a satisfactory agreement with the correlations of Kuehn and Goldstein (1978) and Raithby and Hollands (1975). He also proposed a new correlation that accounted for the expansion number.

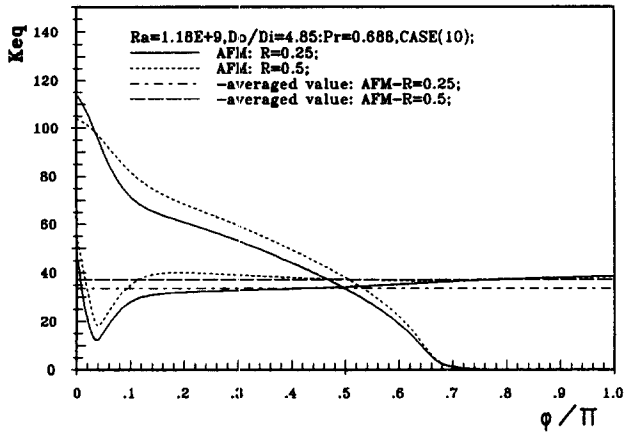

Figure 10 Normalized local Nusselt number around the inner and outer cylinder of a concentric annulus, $D_o/D_i = 4.85$, Ra = 1.18×10^9

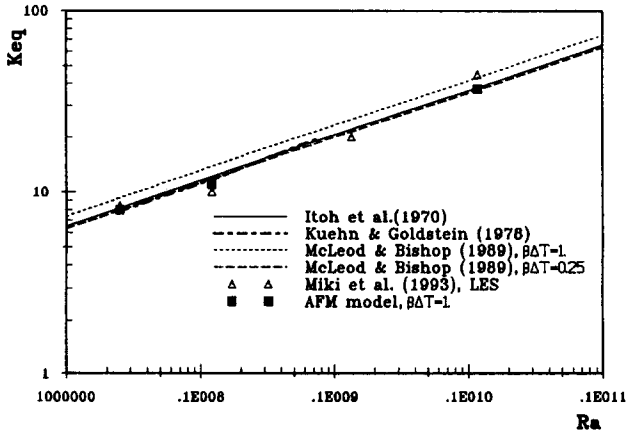

Figure 12 Comparison of the predicted normalized Nusselt numbers K_{eq} with the LES data and some empirical correlations

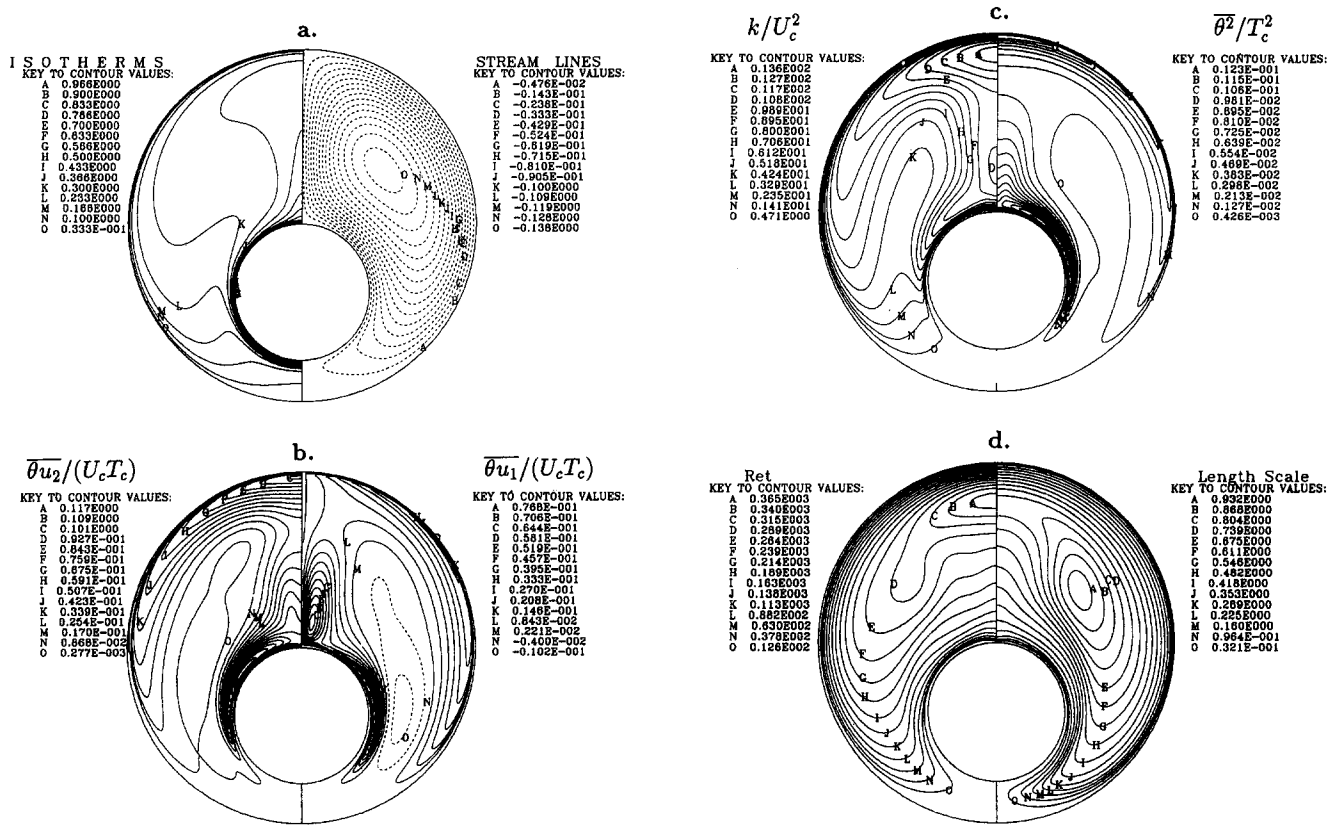

Figure 13 Computed contours of mean flow and turbulence properties in an eccentric annulus, $D_o/D_i = 2.6$, $e/L = -0.623$, $Ra = 2.5 \times 10^6$

Figure 12 compares our computations for three Ra numbers with the the correlations of Itoh et al. (1970), Kuehn and Goldstein (1978), and McLeod and Bishop (1989), the latter for two values of expansion number. Also the results of the LES for several Ra numbers by Miki et al. (1992) are presented for comparison. As seen, the predicted values of the average equivalent conductivity obtained by the AFM k-ε-$\overline{\theta^2}$ model agree very well with the experimental results and correlations selected.

Because the present computations were performed by applying the Boussinesq approximation, a change in the expansion parameter $\beta\Delta T$, while retaining the same Ra number, produced no effect. The test of the hypothesis of Bishop (1988) about the influence of the expansion number requires the use of real fluid density in a momentum equation, instead of linear density–temperature variation as implied by Boussinesq approximation. Although this poses no additional computational effort, the reproduction of the Bishop's experiments at cryogenic temperatures will depend, among other factors, on the accuracy of the correlations for fluid properties over a large range of density and temperature variation, and this task was not pursued further.

Eccentric annuli

The same model was applied to the computations of supposedly turbulent flow in the eccentric configurations discussed earlier (Figures 3 and 4), for the higher Rayleigh number $Ra = 2.51 \times 10^6$ corresponding to the concentric case. The vertical eccentricity showed a marked influence on the level of turbulence at the Ra number considered: moving the inner cylinder upward produced stabilizing effects and damped the turbulence so that the computations with all models gave for $e/L = +2/3$ invariably laminar solutions regardless of the initial turbulence field. Contrary to that, displacing the inner cylinder downward enhanced the turbulence and generated a different flow pattern, as shown in Figure 13a–d. For example, the maximum turbulent Reynolds number reached the value of about 365, as compared with 200 in the concentric configuration at the same Ra number.

The influence of the eccentricity upon the heat transfer is visible, although not dramatic, at least for the configuration and Ra number considered, Figure 14. On the inner cylinder, the effective Nusselt number is higher all over the surface typically by 20–30%, as compared with the concentric annulus, showing also a more uniform distribution. Along the outer wall, the variation of the Nusselt number is more gradual in the eccentric configuration with the maximum value at the top point considerably lower, but with the averaged value close to that of the concentric annulus. Because of a lack of experimental or other

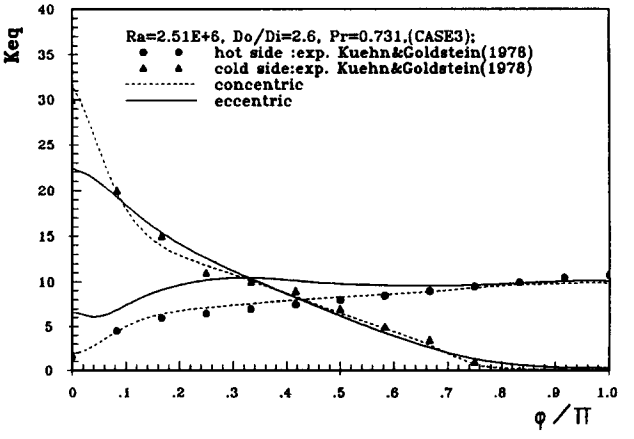

Figure 14 Normalized local Nusselt numbers around the inner and outer cylinder of an eccentric annulus, $D_o/D_i = 2.6$, $e/L = -0.623$, $Ra = 2.5 \times 10^6$

data for this and any other case with a turbulent regime, it was not possible to validate the computed results directly. However, the fact that the laminar flow computation for the same geometry and the turbulent flow computations for the concentric annulus at the same Ra number and diameter ratio agree well with the experiments gives sufficient confidence that the computed results faithfully mimic the actual flow and that the method can be used for predictive purposes in unknown situations.

Conclusions

Numerical study of the turbulent natural convection in horizontal concentric and eccentric annuli with heated inner cylinders, performed by means of a three-equation (k-ε-$\overline{\theta^2}$) algebraic model of turbulence, with incorporated low Re number and wall-proximity effects, yielded generally satisfactory agreement with experimental data and LES by several authors, not only in heat transfer correlation, but also in distribution of mean and fluctuating temperature at several cross sections. The computed flow pattern generally agrees with that detected by optical and other experimental methods. The cases considered included a flow with relatively low Ra number of 2.5×10^6 where the turbulence remains confined to a narrow region around the plume impingement on the outer cylinder. Although the turbulence has a very low intensity (the peak ν_t/ν is only about 16), it makes a noticeable influence on the property distribution and on the local and total Nusselt number, as compared with a purely laminar solution. At higher Rayleigh numbers, the overall agreement of the computations and experiments is even better. In all cases considered, there is a stagnant region below the inner heated cylinder that remains unaffected by the heating. This region increases progressively with an increase in the Rayleigh number, although the turbulence intensity in the upper part of the annulus increases. The computations of the thermal convection in eccentric configuration showed a strong influence on the flow pattern and turbulence field. Displacement of the inner cylinder upward damps the turbulence level as compared with the concentric configuration with the same Ra number and diameter ratio and in the considered case with $D_o/D_i = 2.6$ at $\mathrm{Ra} = 2.5 \times 10^6$ produced complete flow laminarization. In contrast, the displacement of the inner cylinder downward enhances the turbulence level and the overal heat transfer.

The study showed that the application of single-point closure models can yield satisfactory predictions of major flow details relevant to industrial computations. However, to reproduce specific features of the buoyancy-dominated flow recirculation, such as the coexistence of the stagnant fluid, laminar, transitional, and fully turbulent flows in the same domain, it is necessary to employ a higher-order modeling at least at the algebraic-flux level, with the solution of the transport equation for the temperature variance. It is expected that still better results could be expected by solving the transport equations for each component of the turbulent heat flux $\overline{\theta u_i}$ (together with the transport equations for turbulent stresses) and for the temperature variance dissipation rate ε_θ. However, this level of modeling is still associated with a high uncertainty in modeling various terms in the transport equations, and places much higher demands on computer resources. The results discussed here show that the employed general algebraic three-equation method may suffice for the computation of complex industrial flows dominated by natural convection.

Acknowledgments

Most computations reported in the paper have been performed during the stay of S. Kenjereš at the Lehrstuhl für Strömungsmechanik (LSTM) of the Friedrich-Alexander University, Erlangen-Nurember, Germany. The financial support to S. Kenjereš from the International Bureau of the Forschungzentrum, Jülich, Germany, as well as the hospitality of the LSTM are gratefully acknowledged.

References

Bishop, E. H. 1988. Heat transfer by natural convection of helium between horizontal isothermal concentric cylinders at cryogenic temperatures. *J. Heat Transfer*, **110**, 109–115

Demirdžić, I. and Perić, M. 1990. Finite volume method for prediction of fluid flow in arbitrary shaped domains with moving boundaries. *Int. J. Numer., Methods in Fluids*, **10**, 771–790

Fukuda, K., Yasutomi, M. and Hasegawa, S. 1990. Analytical and experimental study on turbulent natural convection in a horizontal annulus. *In. J. Heat Mass Transfer*, **33**, 629–639

Galpin, P. F. and Raithby, G. D. 1986. Numerical solution of problems in incompressible fluid flow: Treatment of the temperature–velocity coupling. *Numer. Heat Transfer*, **10**, 105–129

Grigull, U. and Hauf, W. 1966. Natural convection in horizontal cylindrical annuli. *Proc. 3rd Int. Heat Transfer Conf.*, **2**, 182–195

Grötzbach, G. and Wörner, M. 1992. Analysis of second-order transport equations by numerical simulations of turbulent convection in liquid metals. *Proc. 5th Int. Topical Meeting on Nucl. Reactor Thermal Hydraulics, NURETH-5*, Sept. 1994, Salt Lake City, UT, **2**, 358–365

Hanjalić, K. 1994. Achievements and limitations in modeling and computation of buoyant turbulent flows and heat transfer. Special keynote lecture, *10th Int. Heat Transfer Conf.*, 14–18 August, 1994, Brighton, UK

Hanjalić, K., Kenjereš, S. and Durst, F. 1995. Natural convection in partitioned two-dimensional enclosures at higher Rayleigh numbers. *Int. J. Heat Mass Transfer*, to appear

Ince, N. Z. and Launder, B. E. 1989. On the computation of buoyancy-driven turbulent flows in rectangular enclosures. *Int. J. Heat Fluid Flow*, **10**, 110

Itoh, M., Fujita, T., Nishiwaki, N. and Hirata, M. 1970. A new method of correlating heat transfer coefficients for natural convection in horizontal cylindrical annuli, *Int. J. Heat Mass Transfer*, **13**, 1364–1368

Jones, W. P. and Launder, B. E. 1972. Prediction of laminarization with a two-equation model of turbulence. *Int. J. Heat Mass Transfer*, **15**, 301

Kenjereš, S. and Hanjalić, K. 1995. On the prediction of thermal convection in horizontal slender enclosures. *Proc. 10th Symp. Turbulent Shear Flows*, Pennsylvania State Univ., U.S.A

Kuehn, T. H., and Goldstein, R. J. 1976. An experimental and theoretical study of natural convection in the annulus between horizontal concentric cylinders, *J. Fluid Mechanics*, vol. **74**, pp. 695–719

Kuehn, T. H. and Goldstein, R. J. 1978. An experimental study of natural convection heat transfer in concentric and eccentric horizontal cylindrical annuli. *J. Heat Transfer*, **100**, 635–640

Launder, B. E. and Sharma, B. I. 1974. Application of the energy dissipation model of turbulence to the calculation of flow near spinning disc. *Lett. Heat Mass Transfer*, **1**, 131–138

Lis, J. 1966. Experimental investigation of natural convection heat transfer in simple and obstructed horizontal annuli. *Proc. 3rd Int. Heat Transfer Conf.*, **2**, 196–204

McLeod, A. E. and Bishop, E. H. 1989. Turbulent natural convection of gases in horizontal cylindrical annuli at cryogenic temperatures. *Int. J. Heat Mass Transfer*, **32**

Miki, Y., Fukuda, K. and Taniguchi, N. 1993. Large-eddy simulation of turbulent natural convection in concentric horizontal annuli. *Int. J. Heat Fluid Flow*, **14**, 210–216

Raithby, G. D. and Hollands, K. G. T. 1975. A general method of obtaining approximate solutions to laminar and turbulent free convection problems. *Adv. Heat Transfer*, **11**, 265–315

Shabbir, A. and Taulbee, D. B. 1990. Evaluation of turbulence models for predicting buoyant flows. *J. Heat Transfer*, **112**, 945–951

Stone, H. L. 1968. Iterative solution of implicit approximations of multi-dimensional partial differential equations. SIAM, *J. Num. Anal.*, **5**, 530